

# Carbon transport in TCV

A. Zabolotsky<sup>1</sup>, M. Bernard<sup>1</sup>, V. Piffel<sup>2</sup>, H. Weisen<sup>1</sup>, A. Bortolon<sup>1</sup>, B.P. Duval<sup>1</sup>, A. Karpushov<sup>1</sup>

<sup>1</sup>*Ecole Polytechnique Fédérale de Lausanne (EPFL),*

*Centre de Recherches en Physique des Plasmas,*

*Association Euratom-Confédération Suisse, CH-1015 Lausanne, Switzerland*

<sup>2</sup>*Institute of Plasma Physics, Association Euratom-IPP.CR, Prague, Czech Republic*

## Introduction

Knowledge of the impurity transport parameters and their relation with those of the main plasma particles is important for predicting the fusion performance of a tokamak reactor and provides an element for validating advanced transport models currently under development.

The radial profiles of fully ionized carbon  $C^{6+}$  (transition  $n=8-7$ , 529.1 nm) released from TCV ( $R = 0.88$  m,  $a < 0.25$  m,  $B_T < 1.5$  T) wall tiles were measured using active Charge eX-change Recombination Spectroscopy (CXRS) [1]. A 1D impurity transport model was used to infer carbon transport parameters from the steady state profiles of fully ionized carbon. At high  $q_{95}$  a phenomenon of impurity accumulation of anomalous (rather than neoclassical) origin is observed.

## Observations

Charge exchange spectra were obtained in a wide variety of plasma conditions using a diagnostic neutral beam enhanced CXRS signal fitted with a Gaussian profile, taking into account the spectrometer instrumental function. The density of the  $C^{6+}$  along the line of sight was obtained by integrating the fitted active component of the signal corrected for the neutral beam attenuation and the changes of CX rate coefficient along the beam.

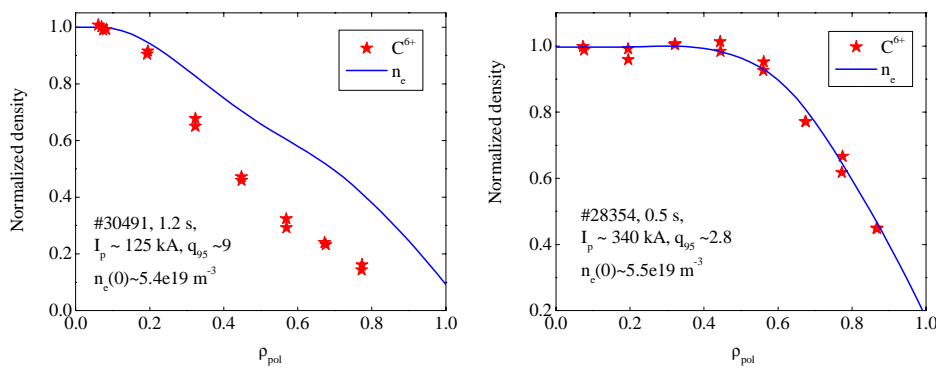


**Fig. 1: Examples of measured profiles in Ohmic discharges with low (left) and high (right) plasma current and mapped on  $\rho_{pol} = \sqrt{\Psi}$  grid ( $\Psi$  is the normalized poloidal flux)**

The resulting normalized profile of  $C^{6+}$  in Ohmic TCV discharges are shown on the Fig. 1. The  $C^{6+}$  profiles are peaked and in the case of the low current plasma discharge they are significantly more so that the electron density. Fig. 2 shows the dependence of the normalized gradients  $\nabla n_{C^{6+}}/n_{C^{6+}}$  for  $C^{6+}$  and  $\nabla n_e/n_e$  at  $\rho_{pol}=0.5$  on the parameter  $\langle j \rangle / j_0 q_0$  which is a

generalization of the parameter  $1/q_{95}$  for non circular plasmas. The parameter  $\langle j \rangle / j_{0q0}$  is known to provide a scaling for electron density gradient in TCV Ohmic plasmas [2].

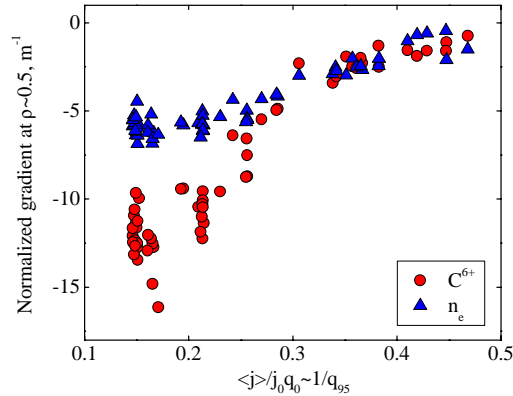


**Fig. 2 Normalized gradients  $\nabla n / n$  of  $C^{6+}$  measured by CXRS and of electron density profiles from TS at  $\rho_{pol} = 0.5$**

As already noticed in Fig 1 in low current Ohmic discharges, the  $C^{6+}$  profiles are more peaked than the electron density profiles and for the high current discharges ( $q_{95} < 4$ ) the normalized gradients of  $C^{6+}$  and of  $n_e$  become similar. The region of  $\langle j \rangle / j_{0q0}$ , in which gradients of  $C^{6+}$  are higher than electron density gradients, is characterized by the absence of sawtooth activity. The scaling of normalized  $C^{6+}$  gradients does not depend on the absolute value of the electron density or temperature. Dependences on other parameters such as shape, collisionality have not yet investigated. Measurements of  $C^{6+}$  were also performed in low current ( $q_{95} > 5$ ) L-mode ECRH discharges. In ECRH discharges the  $C^{6+}$  density gradients are on average somewhat lower than in Ohmic discharges, but higher than the electron density gradients.

## Simulations

Carbon transport parameters in steady state were obtained by means of the STRAHL code [3]. STRAHL is a one dimensional transport code which calculates the solution of the equation of impurity particle continuity for each ionisation stage:  $\frac{\partial n_{i,z}}{\partial t} = -\vec{\nabla} \Gamma_{i,z} + Q_{i,z}$ , where  $\Gamma_{i,z}$  is the flux density of the impurity and  $Q_{i,z}$  is the source/sink term, which includes ionisation, radiative, dielectronic and charge exchange recombination from and to the neighbouring ionisation stages. The impurity flux density is represented in the conventional form as a sum of diffusive and convective terms:  $\Gamma_z = -D \nabla n_z + V n_z$ , where  $D$  is the diffusion coefficient and  $V$  is the pinch velocity, which is negative for inward convection. Background electron temperature and density profiles used in the simulations were taken from the Thomson scattering system. For modelling, trial profiles of  $D$  and  $V$  are provided to the code as input parameters and normalized profiles of all ionisation stages are obtained as the output.

In order to understand the role of the convection term for carbon in the particle balance equation, scans of  $D$  (constant as a function of  $\rho$ ) with  $V = 0$  were performed. Impurity confinement times were obtained by fitting with the exponential the decay of carbon concentration after switching off the edge carbon source in the simulation. The results of  $D$  scans for the

low and high current discharges are shown on Fig. 3. For the lowest values,  $D=0.2 \text{ m}^2/\text{s}$ , the simulated profiles are too flat with respect to the measured profile. It is seen that even for  $D=15 \text{ m}^2/\text{s}$ , the simulated profiles of  $C^{6+}$  cannot fit the measured profile at low current, only reproducing the profile at high current. However with such high values of  $D$ , the carbon confinement time is  $\sim 1 \text{ ms}$ , which is significantly less than the energy confinement time ( $\tau_e \sim 14 \text{ ms}$ ) and Si confinement time,  $\sim 20\text{-}50 \text{ ms}$ , measured in similar conditions using laser blow-off [4]. Therefore an inward pinch is unavoidable for reproducing the measured profiles of  $C^{6+}$ , when constraining confinement times to be consistent with observations.

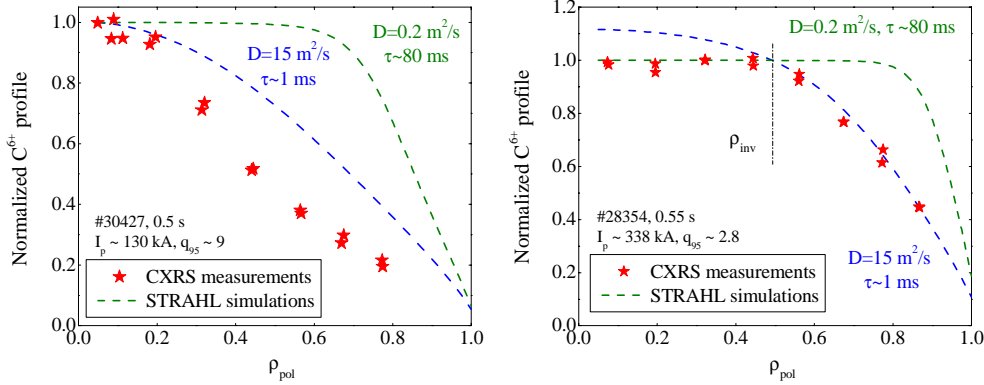


**Fig. 3 Profiles of  $C^{6+}$  measured by CXRS (stars) and simulated by STRAHL (dashed lines) using flat  $D$  profiles and  $V = 0$  for low (left) and high (right) current discharges. The vertical line on the right figure indicates the position of sawtooth inversion radius.**

To find the carbon transport coefficients for the discharges on Fig. 3 the iteration method was used. The profiles of  $D$  were approximated by a parabolic function  $D=D_0\rho^2+0.25$  according to the results presented in Ref. [5]. Profiles of  $V$  were defined by smoothly connecting 5 nodal points along the minor radius. The best fitting  $V$  was found by independently scanning the node values. For each best fitting profiles given by the pair  $D$  and  $V$ , the confinement time was calculated and the value  $D_0$  was changed. Iterations continued until the confinement time of 20 ms was obtained. The resulting profiles of  $C^{6+}$  simulated by STRAHL, together with the best fitting profiles  $D$  and  $V$  are shown on Fig. 4. Comparing the best fitting values of  $V$  in high and low current discharges one can conclude that the dependence of the carbon gradient on  $\langle j \rangle / j_{0q_0}$  is due to the changes of the convection rather than changes of the diffusion. STRAHL simulations also indicate that partly ionized stages of carbon are outside the region  $\rho_{\text{pol}} \sim 0.6$  and therefore the scaling for  $C^{6+}$  normalized gradients presented on Fig. 2 is also valid for the total C density gradients.

The best fitting values of  $D$  and  $V$  were also compared with the neoclassical transport coefficients calculated by the NEOART module [3].  $D_{\text{neo}}$  and  $V_{\text{neo}}$ , obtained as the sum of classical, banana and Pfirsch – Schlüter transport coefficients, are shown on Fig. 4 by dashed lines. The comparison shows that diffusion coefficients are always anomalous, whereas the pinch velocity is clearly anomalous only for low current Ohmic discharges where carbon profiles are most peaked. For the flatter carbon profile in the high current TCV discharge, the best fitting values of  $V$  is close to the neoclassical level.

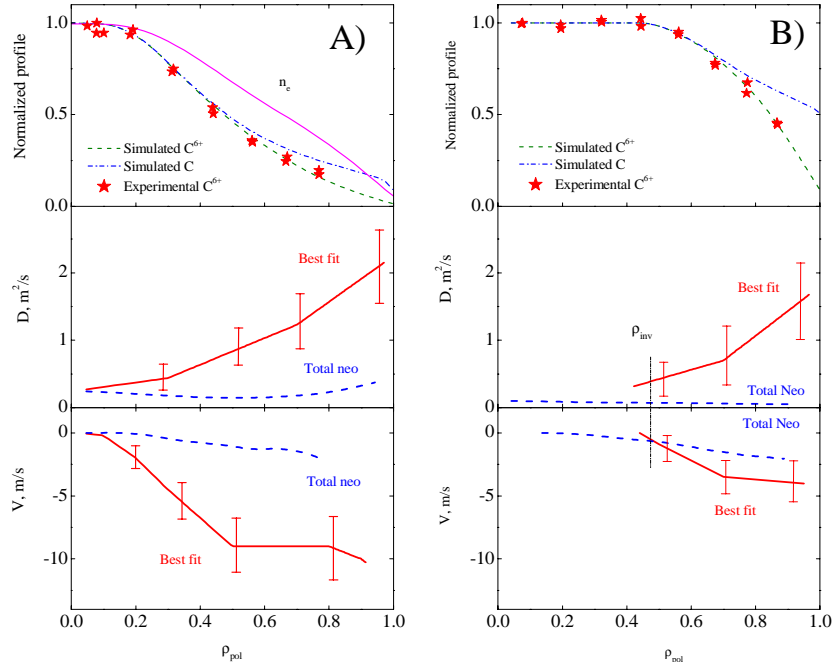


**Fig. 4** Experimental and simulated profiles of carbon, as well as best fitting values of  $D$  and  $V$ , together with neoclassical coefficients for the discharges presented on Fig 3.

## Conclusions

Observations show that in stationary Ohmic and ECR heated L-mode discharges, the profiles of carbon are always peaked, with a clear dependence of  $\nabla n_c/n_c$  on  $\langle j \rangle / j_0 q_0$  in OH discharges. For  $q_{95} > 4$ ,  $|\nabla n_c/n_c| > |\nabla n_e/n_e|$ , whereas for  $q_{95} < 4$   $|\nabla n_c/n_c| \cong |\nabla n_e/n_e|$ . The STRAHL simulations unambiguously indicate the presence of inward pinch for carbon in Ohmic as well as in ECRH discharges. The best fitting transport coefficients of  $D$  and  $V$  are found to be anomalous, with  $V$  approaching the neoclassical level at low  $q_{95}$ .

The observed peaking of the carbon density profiles at high  $q_{95}$ , i.e. exceeding the peaking of the density profiles, is evocative of neoclassical impurity accumulation. Remarkably, the measurements described show that its origin is anomalous, rather than neoclassical.

## Acknowledgement

This work was partly supported by the Swiss National Science Foundation and by the Academy of Sciences of the Czech Republic, AVOZ 20430508.

## References

- [1] A. N. Karpushov et al., *Fusion Eng. Des.* **66–68** (2003), 899–904
- [2] A. Zabolotsky, H. Weisen and TCv Team, *Plasma Phys. Control. Fusion* **45** (2003), 735
- [3] R. Dux. STRAHL User Manual, IPP Garching, Germany  
<http://www.rzg.mpg.de/~rld/strahl.ps>
- [4] E. Scavino et al., *Plasma Phys. Control. Fusion* **45** (2003) 1961
- [5] V. Piffel et al., *Plasma Phys. Control. Fusion* **46**, (2004), 1659